Adlayer Structures and Electrocatalytic Activity for O_2 of Metallophthalocyanines on Au(111): In Situ Scanning Tunneling Microscopy Study

Soichiro Yoshimoto,† Akinori Tada,† Koji Suto,† and Kingo Itaya*,†,‡

Department of Applied Chemistry, Graduate School of Engineering, Tohoku University, Aoba-yama 04, Sendai 980-8579, Japan, and CREST-JST, Kawaguchi Center Building, 4-1-8 Honcho, Kawaguchi City, Saitama 332-0012, Japan

Received: December 25, 2002; In Final Form: April 11, 2003

Adlayers of cobalt(II) and copper(II) phthalocyanines (CoPc and CuPc) prepared on Au(111) from CoPc- and CuPc-saturated benzene solutions were investigated in 0.1 M $HClO_4$ by using cyclic voltammetry and in situ scanning tunneling microscopy (STM). The CoPc-modified Au(111) electrode was found to enhance the electrochemical reduction of O_2 to H_2O_2, whereas the CuPc-modified Au(111) electrode showed no electrocatalytic activity for O_2 reduction. High-resolution STM images revealed the characteristic shape, internal structure, and orientation of each CoPc and CuPc molecule in ordered domains. Both CoPc and CuPc molecules formed three packing arrangements on Au(111) surface, i.e., one rectangular arrangement on reconstructed Au(111) and two hexagonal arrangements on Au(111)−(1 × 1), depending on the surface coverage. The center cobalt ion in CoPc appeared as the brightest spot in the STM image, whereas the copper ion in CuPc appeared as a dark spot.

Introduction

Formation and characterization of ordered adlayers of porphyrins and phthalocyanines at electrolyte−electrode interfaces are important from the fundamental and technological points of view. Phthalocyanines are of great interest in such diversified fields as biology,[1] photosynthesis,[1] electrocatalysis,[2] and molecular devices.[3] For example, copper(II) phthalocyanine (CuPc) was applied to devices such as light emitting diodes (LED)[4] and field effect transistors (FET).[3,4] In electrochemistry, thin films of metallophthalocyanines (MPcs) have been intensively studied for the interest in electrocatalytic reactions, such as the reduction of O_2 for developing efficient cathode materials of fuel cells.[5−9] For the electrochemical catalytic reduction of O_2, the reactivity has been mainly investigated on graphite electrodes modified with various MPcs[7−9] and their derivatives such as 4,4,4,4-tetrasulfonate and 4,4,4,4-tetraamino CoPcs.[9] However, not much attention has been paid so far to the adlayer structure of those MPcs on electrode surfaces. The relationship between the adlayer structure and the electrocatalytic activity has not yet been clarified.

Structures of MPc adlayers on various metal surfaces have been studied using scanning tunneling microscopy (STM) mostly in UHV.[10−14] Lippel et al. reported the first STM images of CuPc adlayer on Cu(100).[10] Hipps and co-workers reported various metal-coordinated Pcs such as CuPc,[12,13] CoPc,[12,13] NiPc,[14] FePc,[14] and VOPc[15] on Au(111) in UHV. More recently, the adsorption of nonplanar SnPc on the Ag(111) surface was also studied in UHV by Lackinger et al.,[16] in which the central Sn metal was found to be pointing either toward or off the Ag surface, reflecting the arrangement of SnPc molecules on Ag(111).

MPc layers have also been studied on surfaces other than metals. Strohmaier et al. studied PbPc on MoS_2 in UHV.[17] Bai and co-workers investigated alkyl-substituted CuPc and ZnPc layers formed on highly ordered pyrolytic graphite (HOPG),[18] CuPc layers on *n*-alkane-adsorbed HOPG,[19] and copper(II) 2,3,9,10,16,17,23,24-octakis(carboxyl)-29*H*,31*H*-phthalocyanine on stearic acid-covered HOPG in ambient atmosphere.[20]

STM has been widely accepted as a tool for studying the structure of adlayers also in solution.[21−29] We previously reported that highly ordered arrays of water-soluble 5,10,15,-20-tetrakis(*N*-methylpyridinium-4-yl)-21*H*,23*H*-porphine (H_2-TMPyP) molecules were formed on the iodine-modified (I−) Au(111),[21−23] I−Ag(111),[24] and I−Pt(100),[25] and sulfur-modified Au(111)[26] electrodes in solution. In addition to symmetry and structure of the H_2TMPyP array, the STM image reveals a great deal of information concerning the internal molecular structure. Tao et al. also investigated the adlayers of three water-soluble molecules, iron(III) protoporphyrin (IX), zinc(II) protoporphyrin (IX), and protoporphyrin (IX), on the graphite basal plane in aqueous solutions with both STM[28,29] and atomic force microscopy (AFM).[28] Similar adlayer structures were formed among three molecules, although the internal structures obtained by in situ STM were significantly different.[28]

As listed above, STM imaging of hydrophobic MPc molecules was successful in UHV[10−17] and in air;[18−20] however, the number of reports on adlayer structures of MPc in aqueous electrolyte solutions is still small mainly because of their low solubility in aqueous solutions. Very recently, we succeeded in forming highly ordered molecular arrays of water-insoluble tetraphenyl-21*H*,23*H*-porphine cobalt(II) (CoTPP) and copper-(II) (CuTPP) spontaneously on Au(111) surfaces by immersing Au(111) in benzene solutions containing those molecules.[30] Thus-formed adlayers of CoTPP and CuTPP were observed in $HClO_4$ solution, and the structures were found to be identical to those previously observed in UHV.[31,32] Because benzene does

* To whom correspondence should be addressed. E-mail: itaya@atom.che.tohoku.ac.jp. Phone/Fax: +81-22-214-5380.
† Tohoku University.
‡ CREST-JST.

10.1021/jp027825a CCC: $25.00
Published on Web 05/28/2003

CHART 1: Chemical Formula of Metal(II) Coordinated Phthalocyanine (MPc, M = Co or Cu)

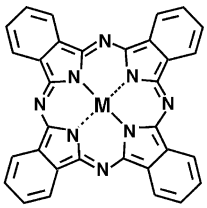

not adsorb on the Au(111) surface, adlayers of water-insoluble aromatic molecules are formed without interference of the adsorption of benzene.[33] This method for the preparation of ordered adlayers using benzene solutions is also expected to be applicable to the investigation of adlayers of MPcs on the Au(111) surface.

In the present paper, we report adlayer structures of CoPc and CuPc molecules (see Chart 1) formed on a Au(111) electrode surface. Clear dependency of adlayer structures of CoPc and CuPc on immersion time was found on Au(111) surfaces in the present study. Adlayer structures of CoPc and CuPc formed on Au(111) were found to transform themselves to other structures with an increase in immersion time. Packing arrangements of CoPc and CuPc formed on Au(111) were accurately determined in 0.1 M $HClO_4$, and even internal structures were clearly revealed by high-resolution STM.

Experimental Section

CoPc and CuPc were obtained from Aldrich. Benzene (Spectroscopy Grade) was purchased from Kanto Chemical Co. The CoPc- or CuPc-saturated benzene solution was prepared by ultrasonicating for 10 min. The aqueous electrolyte solution was prepared with $HClO_4$ (Cica-Merck) and ultrapure water (Milli-Q SP-TOC; $\geq$ 18.2 MΩ cm).

The Au(111) single-crystal electrode was prepared by the Clavilier method.[34] It was annealed in hydrogen flame and quenched into ultrapure water saturated with hydrogen.[35] A thermally reconstructed Au(111)$-(p \times \sqrt{3})$ surface was also used in the present study. CoPc adlayers were formed by immersing the Au(111) electrode into a benzene solution saturated with CoPc for 5−20 min. The CoPc-adsorbed Au(111) electrode was then rinsed with ultrapure water to prevent contamination, and it was transferred into an electrochemical cell for voltammetric and STM measurements. The same procedure was used to prepare CuPc adlayers on well-defined Au(111) electrodes, but a much longer immersion time (more than 20 h) was required because of the lower solubility of CuPc than that of CoPc.

Cyclic voltammetry was carried out at 20 °C using a potentiostat (HOKUTO HAB-151, Tokyo) with the hanging meniscus method in a three-compartment electrochemical cell in N_2 atmosphere. The catalytic activity of the CoPc- and CuPc-modified Au(111) electrodes for the reduction of O_2 was examined in 0.1 M $HClO_4$ saturated with O_2. Electrochemical STM measurements were performed by using a Nanoscope E (Digital Instruments, Santa Barbara, CA) with tungsten tips etched in 1 M KOH. To minimize the residual faradic current, the tips were coated with nail polish. STM images were taken in the constant-current mode. All potentials are referred to the reversible hydrogen electrode (RHE).

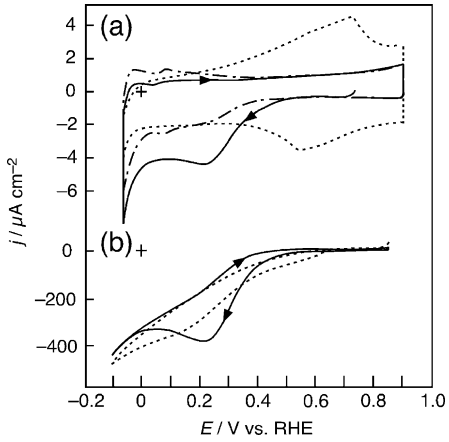

Figure 1. Typical cyclic voltammograms of bare (dotted lines) and CoPc-adsorbed (solid lines) Au(111) electrodes in 0.1 M $HClO_4$ under N_2 atmosphere (a) and O_2 atmosphere (b). The dashed line in Figure 1a was obtained in the second scan of CoPc-modified Au(111). The potential scan rate was 50 mV s^{-1}.

Results and Discussion

Voltammetry. Figure 1 shows typical cyclic voltammograms (CVs) of bare (dotted lines) and CoPc-adsorbed (solid lines for the first scan and dashed lines for the second scan) Au(111) electrodes in 0.1 M $HClO_4$ at a scan rate of 50 mV s^{-1}. The CoPc-adsorbed Au(111) sample was obtained by immersion in a benzene solution of CoPc for 10 min. The open circuit potential (OCP) of a well-defined Au(111) electrode in 0.1 M $HClO_4$ was in the range of 0.7−0.75 V. The voltammogram for the bare Au(111) in Figure 1a in the double-layer potential region is identical to that reported previously,[33] which shows that a well-defined Au(111) surface was exposed to the $HClO_4$ solution. The CV profile of a Au(111) electrode immersed in pure benzene for 10−60 s and rinsed with ultrapure water was essentially the same as that observed on a clean, fresh Au(111) electrode.[33] This result indicates that benzene does not adsorb on the Au(111) surface in the present conditions.

After the preparation of a CoPc adlayer by immersion of Au(111) in a benzene solution saturated with CoPc for 10 min, the OCP of the CoPc-adsorbed Au(111) electrode was in the range of 0.75−0.85 V. The potential scan was then started in the negative direction from the OCP in the double-layer region (solid line). The decrease in the double-layer charging current in Figure 1 clearly shows that the Au(111) surface is covered with hydrophobic CoPc molecules. The repetitive potential cycling between 0.5 and 0.9 V caused no change in the CV profile, suggesting that the CoPc adlayer formed on Au(111) is stable in the double-layer potential range. As can be seen in Figure 1, a reductive peak appeared at 0.22 V during the first cathodic scan (solid line). The increase in cathodic current commencing at −0.05 V is due to the H_2 evolution reaction. On the other hand, an oxidation peak was hardly seen during the first anodic scan (solid line). As described in our recent paper, the reductive current from Co(III) to Co(II) was observed at 0.32 V on a CoTPP-modified Au(111) electrode.[30] The reduction peak at 0.22 V during the cathodic scan shown in Figure 1a is thus thought to be associated with the reduction of Co(III) to Co(II) in CoPc adsorbed on Au(111). The second scan shown by the dashed lines in Figure 1a is different from the first scan: the cathodic current for the reduction of Co(III) to Co(II) observed in the first scan (solid line) at 0.22 V is no longer seen. The CVs in Figure 1a appear to indicate that the reoxidation process of Co(II) to Co(III) is very slow and that the CoPc molecules after the first cathodic scan remain mostly

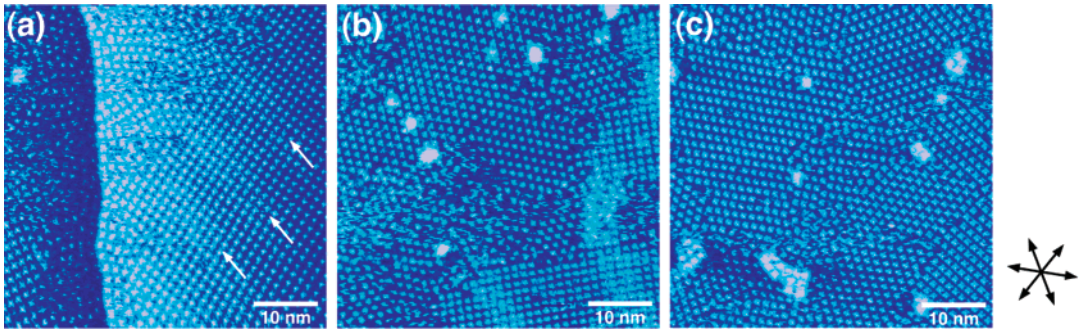

Figure 2. Large-scale (50 × 50 nm^2) STM images of a CoPc adlayer formed on Au(111) acquired in 0.1 M $HClO_4$ at 0.85 V versus RHE. The adlayer was prepared by immersion in benzene solution saturated with CoPc for 5 (a), 10 (b), and 20 min (c). The potential of the tip and the tunneling currents were 0.35 V and 10 nA, respectively. The set of three arrows indicates the close-packed directions of the Au(111) substrate.

in the reduced form with Co(II) on Au(111). The total cathodic charge density in the first scan consumed for the peak at 0.22 V in Figure 1a was calculated to be 7.8 ± 0.4 μC cm^{-2}, which is equivalent to (8.1 ± 0.4) × 10^{-11} mol cm^{-2}. This value indicates that CoPc forms a monolayer on the Au(111) surface. The difference in reductive peak potentials between CoPc and CoTPP, 0.22 and 0.32 V, respectively, could probably be explained by the difference in metal ligand interaction, electronic structure[6,7] and/or adlayer structure.

Figure 1b shows cyclic voltammograms obtained in 0.1 M $HClO_4$ saturated with O_2. On the bare Au(111) electrode (dotted line), a cathodic current due to the reduction of O_2 commenced at ca. 0.6 V, and it gradually increased in the potential range between 0.6 and −0.1 V. On the CoPc-adsorbed Au(111) electrode (solid line), the reduction current of O_2 commenced at ca. 0.45 V during the cathodic scan, and a clear electrocatalytic reduction peak of O_2 was found at ca. 0.2 V, indicating that the CoPc adlayer catalyzes the reduction of O_2. At more negative potentials than 0.2 V, the reductive current remained almost constant because of the limitation of the diffusion of O_2. The CV profile for the CoPc-modified Au(111) electrode was stable during repetitive cycles between −0.1 and 0.85 V; the CoPc thin film formed on Au(111) was not desorbed in this potential range. It was roughly estimated from the current density (ca. 0.4 mA cm^{-2}) that the two-electron reduction from O_2 to H_2O_2 occurred on the CoPc-adsorbed Au(111) electrode. This current density for the reduction peak was comparable to that on the CoTPP-modified Au(111) electrode.[30]

The immersion time for Au(111) in the benzene solution containing CoPc was varied from 5 to 30 min. The CoPc-modified Au(111) samples thus prepared with different immersion times exhibited the same CV profiles as those of the sample prepared by immersion in the benzene solution for 10 min, both in pure (Figure 1a) and O_2-containing (Figure 1b) $HClO_4$ solutions.

The reduction of O_2 on the CuPc-modified Au(111) electrode was also examined (not shown). At the CuPc-modified Au(111) electrode, the reduction current of O_2 was depressed, and the current started to flow only at potentials more negative than ca. 0 V. According to the previous papers, the electrocatalytic activity of the MPc-modified electrodes for the reduction of O_2 was in the order of Fe(II) > Co(II) ≥ Ni(II) > Cu(II) ≈ 0.[6,7] The difference in electrocatalytic activity for the reduction of O_2 has been explained by back-bonding, i.e., interaction of the filled oxygen orbitals with the vacant d_{z^2} orbital of the center metal.[6]

In Situ STM. *(1) CoPc Adlayers.* To understand the formation of a CoPc adlayer on the Au(111) surface, CoPc adlayers were prepared on the Au(111) surface with various immersion times. Figure 2a−c shows typical STM images of CoPc adlayers formed on Au(111) by immersing the substrate for 5, 10, and 20 min in the benzene solution, respectively. As can be seen in Figure 2a, for the immersion time of 5 min, well-ordered bright spots with square symmetry were observed on the entire surface of the terrace. Each CoPc molecule can be clearly recognized as a bright spot not only on atomically flat terraces but also near the step. Under the conditions of this experiment, terraces were entirely covered with CoPc molecules. Interestingly, modulation is seen as rows on the surface in Figure 2a. Careful inspection of the Au(111) surface reveals that rows indicated by arrows in Figure 2a are separated with a spacing ranging from ca. 6 to 9 nm on the terrace. The difference in height is only ca. 0.06 nm, which is much smaller than that of the atomic step. These results reveal that the transformation of underlying Au atoms from (1 × 1) to ($\sqrt{3}$ × 22), or the so-called reconstruction, was caused by the adsorption of CoPc. In the UHV environment, CoPc layers have already been reported to be formed on the reconstructed Au(111) surface prepared previously as ($\sqrt{3}$ × 22),[12,13] whereas the reconstruction from (1 × 1) to ($\sqrt{3}$ × 22) which proceeded upon adsorption of CoPc is a new finding of this study. We also carried out the adsorption of CoPc onto a thermally reconstructed Au(111) surface. The image obtained was essentially the same as that shown in Figure 2a.

In general, Au(111) retains its (1 × 1) structure after the adsorption of organic compounds such as coronene,[33,36] fullerene C_{60}, and fullerene dimer C_{120}[37] near the OCP. It is surprising that reconstruction of the Au(111) surface from (1 × 1) to ($\sqrt{3}$ × 22) was induced by adsorption of CoPc during immersion in the benzene solution, and that the reconstruction took place even in the aqueous solution at potentials near the OCP. The reason for the reconstruction being induced by the adsorption of CoPc is not clear, but the following mechanism may be proposed: the adsorbed CoPc probably induces a negative charge on the Au(111) surface so that the potential of zero charge (E_{pzc}) of the CoPc-adsorbed Au(111) shifts to a value more positive as has been noted for bare Au(111) (0.24 V vs SCE) in 0.01 M $HClO_4$.[38] The reconstruction of the Au(111) surface has been shown to be induced also by the adsorption of CoTPP and CuTPP as reported in our recent paper.[30]

When the modification by CoPc was carried out for 10 min, another domain newly appeared on the terrace as shown in Figure 2b. It is clearly seen that the terrace was covered with two different domains, square and hexagonal. Interestingly, in the hexagonal packing region, no reconstructed rows of Au(111) were seen, and the (1 × 1) structure of Au(111) reformed under the molecular layer of hexagonal regions. Several small islands appeared in the hexagonal regions on the terrace as

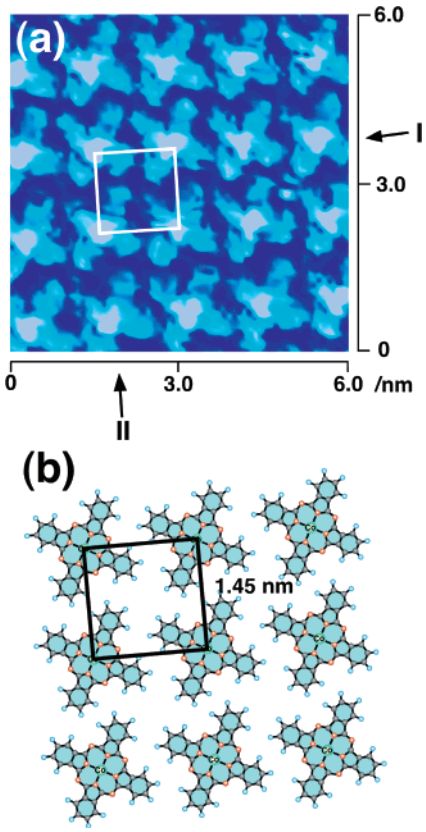

Figure 3. High-resolution STM image (6×6 nm^2) of a CoPc adlayer formed on a reconstructed Au(111) surface acquired in 0.1 M $HClO_4$ at 0.85 V versus RHE (a) and a structural model (b). The potential of the tip and the tunneling current were 0.45 V and 10 nA, respectively.

shown mainly in the upper part of Figure 2b. The average height of each island was approximately 0.25 nm, which is close to that of a monatomic step. These islands with an atomic height might have been formed as a result of the lifting of reconstruction, namely, from ($\sqrt{3} \times 22$) to (1×1). The formation of such islands on Au(111) was previously reported in H_2SO_4 in the presence of uracil in a rather positive potential region.[39] According to the paper, uracil formed a chemical bond between the N atom in each uracil molecule and Au(111) substrate as a result of the deprotonation of the uracil molecule.[39] In the case of the CoPc adlayer formed on reconstructed Au(111), it is assumed that the lifting of reconstruction took place with an increase in surface concentration of CoPc and a strong interaction between CoPc molecules and Au(111) lattice, which will be discussed later. When the immersion time was longer than 20 min, the terrace was completely covered with hexagonal ordered domains without square domains (Figure 2c). No reconstructed rows were found, indicating that the phase transition of underlying Au atoms resulting from the lifting of reconstruction to (1×1) was accomplished because of an increase in the surface concentration of CoPc. A typical domain size of CoPc formed on the Au(111)$-(1 \times 1)$ surface was 10∼15 nm. Careful inspection of the highly ordered arrays of the CoPc molecule formed on the Au(111)$-(1 \times 1)$ reveals that islands are often observed at domain boundaries as shown in Figure 2c.

Figure 3a shows a typical high-resolution STM image of a CoPc adlayer taking a square arrangement, which was acquired in an area of 6×6 nm^2. The adlayer of CoPc was prepared by immersion for 5 min. The CoPc molecular array is two-dimensionally well organized. Each CoPc molecule can be recognized as a propeller-shaped image with the brightest spot at the center and four additional bright spots at the corners of each molecule. The brightest spot at the center and the four additional spots can be attributed, respectively, to the cobalt ion and the benzene rings in the CoPc molecule with a flat-lying orientation. As seen in the STM images obtained in UHV by Hipps' group,[12,13] the center of each CoPc molecule was observed as the brightest spot. The molecular shape in the image is reminiscent of the structure of the CoPc molecule (Chart 1). Molecular rows, which are marked by arrows I and II in Figure 3a, cross each other at an angle of approximately 90°. The intermolecular distance between CoPc molecules was found to be 1.45 ± 0.05 nm. Clearly, all CoPc molecules in the adlayer possess the same orientation. The packing arrangement of CoPc observed in the present study in solution was also consistent with that obtained in UHV by Lu et al.[12,13] The packing arrangement of CoPc on Au(111) in Figure 3a is also similar to that of the CoTPP adlayer formed on the Au(111) surface either in UHV[31,32] or in solution,[30] although the lattice of the CoPc parameter was slightly different form that of CoTPP. The unit cell is superimposed in Figure 3a. Each unit cell includes one CoPc molecule, which leads to a surface concentration of ca. 7.9×10^{-11} mol cm^{-2}. The surface concentration estimated from the STM image is in agreement with that obtained from the voltammogram of Figure 1, 8.1×10^{-11} mol cm^{-2}. A structural model for the CoPc lattice is depicted in Figure 3b. The exact relationship between the CoPc adlayer and the underlying Au(111) lattice could not be determined in the present study. According to the model in Figure 3b, the square adlayer of CoPc is incommensurate with respect to the Au-(111) lattice.

CoPc arrays having a well-ordered square lattice were consistently observed in the potential range between 0.1 and 0.9 V. When the potential was held at a potential lower than 0.1 V, the well-ordered arrays of CoPc gradually became smaller, possibly because CoPc molecules became mobile on the Au(111) surface at this potential. At −0.1 V, only a reconstructed Au(111) surface was seen, indicating that CoPc was desorbed from the Au surface. Upon returning the electrode potential from −0.1 to 0.3 V, readsorption of CoPc took place immediately on the Au(111) surface, and a highly ordered square molecular array was again formed on the reconstructed Au-(111) surface. When the electrode potential was scanned to a value more positive than 0.9 V, the highly ordered arrays became unclear, and the lifting of reconstruction from ($\sqrt{3} \times 22$) to (1×1) was observed. This might be due to the oxidation or a structural change of CoPc at very positive potentials.

Figure 4 shows a typical STM image of a CoPc adlayer formed on the Au(111)$-(1 \times 1)$ surface, which was acquired at 0.85 V in 0.1 M $HClO_4$. This CoPc adlayer was prepared by immersing Au(111) in the benzene solution for 20 min. Reconstructed rows of Au(111) under highly ordered arrays of CoPc were no longer seen under the preparation conditions used. Highly ordered hexagonal arrays of CoPc were observed consistently on the terrace. In the image acquired in an area of 25×25 nm^2, several domains are seen, in which each CoPc molecule can be recognized as a propeller-shaped image. The domain boundary between two domains, A and B, is indicated by the dashed line. The molecular rows in domains A and B cross each other at the boundary at an angle of 30° within an experimental error of ± 3°. This result indicates that domain A and domain B are not rotational domains, because, in general, rows in rotational domains cross each other at an angle of 60° or 120°. These hexagonal structures of the CoPc adlayers on Au(111)$-(1 \times 1)$ have not been reported in UHV.

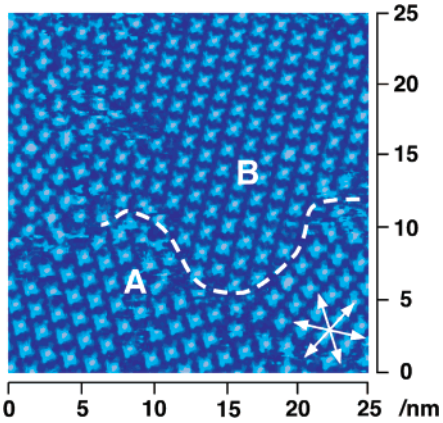

Figure 4. STM image (25×25 nm^2) of a commensurate CoPc adlayer on the Au(111)$-(1 \times 1)$ acquired in 0.1 M $HClO_4$ at 0.85 V versus RHE. Two different domains are labeled A and B, and the domain boundary is marked by the white dashed line. The potentials of the tip and the tunneling current were 0.45 V and 10 nA, respectively. The set of three arrows indicates the close-packed directions of Au(111) substrate.

To clarify structural details of the CoPc adlayer formed on the Au(111)$-(1 \times 1)$ surface, a high-resolution STM image obtained in domain A in Figure 4 is displayed in Figure 5a. Each CoPc molecule can be recognized as a propeller-shaped image with the brightest spot at the center and four additional bright spots at the corners. The adlayer structure of CoPc molecules is in a nearly hexagonal packing arrangement. Molecular rows indicated by arrows I and II were shifted alternately by one-half of the intermolecular distance. Arrows I and II are along the atomic direction of Au(111)$-(1 \times 1)$. The intermolecular spacing in each row along the atomic direction was found to be 1.44 ± 0.03 nm, which corresponds to 5 times the Au lattice constant. The angle between the molecular row indicated by arrow III and the Au(111) lattice direction (dotted line inserted in Figure 5a) was about $3-4°$. A rectangular unit cell is superimposed in Figure 5a. Two CoPc molecules are included in the unit cell with distances of 1.44 ± 0.03 and 3.02 ± 0.08 nm, respectively, for the $[1\bar{1}0]$ direction of Au atomic rows and for the $[\bar{1}12]$ direction, or the so-called $\sqrt{3}$ direction. This distance along the $\sqrt{3}$ direction, 3.02 nm, corresponds to $6\sqrt{3}$ times the Au lattice parameter. The angle between the two unit vectors is 90°. The unit cell of the adlayer structure obtained in Figure 5b is therefore assigned to be $c(5 \times 6\sqrt{3})$*rect*, which yields the surface concentration of 7.7×10^{-11} mol cm^{-2}. A similar packing arrangement was also found in the 5,10,15,20-tetrakis(*N*-methylpyridinium-4-yl)-21*H*,23*H*-porphine (H_2TMPyP) adlayer formed on the I-modified Au(111) surface as described in our previous paper.[21−23]

A high-resolution STM image acquired in domain B is shown in Figure 5b. The scanned area was 6×6 nm^2. Each CoPc molecule can be seen to be propeller-shaped. A precise comparison between this image and that of the underlying Au(111)$-(1 \times 1)$ lattice revealed that all molecular rows are aligned along the $\sqrt{3}$ direction. The molecular rows with side-by-side configuration indicated by arrows I′ and II′ are shifted alternately by one-half of the intermolecular distance. The intermolecular spacing between CoPc molecules (between bright spots at the centers of two molecules) along rows I′, II′, and III′ was measured to be 1.51 ± 0.03 nm, which corresponds to $3\sqrt{3}$ times the Au lattice constant ($3\sqrt{3} \times 0.289$ nm). The unit cell superimposed in Figure 5b is thus determined to be $(3\sqrt{3} \times 3\sqrt{3})$R30°, which leads to the surface concentration of 8.5×10^{-11} mol cm^{-2}.

Height-shaded plots of the data for parts a and b of Figure 5 are shown in parts c and d of Figure 5, respectively. The molecular shape in the image reminds one of the chemical formula of CoPc (Chart 1). Details of the symmetry and even the internal structure of benzene rings of each CoPc molecule can be observed in parts c and d of Figure 5. The ratio of domains composed of $c(5 \times 6\sqrt{3})$*rect* and $(3\sqrt{3} \times 3\sqrt{3})$R30° structures was about 4:6. The average surface concentration of CoPc molecules forming the two adlayer structures on Au(111)$-(1 \times 1)$ can thus be calculated to be ca. 8.1×10^{-11} mol cm^{-2}.

Figure 6a shows a structural model for the $c(5 \times 6\sqrt{3})$*rect* adlayer of CoPc on Au(111)$-(1 \times 1)$. To establish the model, it was necessary to consider the adsorption site of each CoPc molecule. From geometric considerations, we soon found that it is not possible to locate every CoPc molecule at either on-top or 3-fold hollow site but that all CoPc molecules can fit at bridge sites. Bridge sites having a 2-fold symmetry allow us to form two types of geometry, types A and B, as shown in Figure 6a: the only difference between the two types is that a molecule of type A and that of type B are rotated by 90° with respect to each other. Molecules of types A and B are arranged side-by-side in this model (Figure 5a). Surface geometry dictates that three rotational domains must exist in the $c(5 \times 6\sqrt{3})$*rect* symmetry, which was found in our STM imaging. Figure 6b shows a model for the $(3\sqrt{3} \times 3\sqrt{3})$R30° adlayer on Au(111)$-(1 \times 1)$. Molecules of CoPc could be assigned to any site in the $(3\sqrt{3} \times 3\sqrt{3})$R30° symmetry. We tentatively assigned CoPc molecules to a bridge site as well as in the $c(5 \times 6\sqrt{3})$*rect* symmetry.

Let us recall now that when the immersion time in the benzene solution was short (ca. 5 min) the Au lattice was reconstructed and the adlayer of CoPc was incommensurate with respect to the Au lattice (Figure 3). On the other hand, when the immersion time was long (ca. 20 min), the Au lattice became (1×1) and commensurate CoPc layers formed (Figures 4 and 5), with a slight increase in coverage by ca. 3%. These results indicate that the interaction between CoPc and Au substrate might be greater when the adlayers form a $(3\sqrt{3} \times 3\sqrt{3})$R30° or $c(5 \times 6\sqrt{3})$*rect* commensurate structure.

Once the commensurate adlayers were formed on Au(111)$-(1 \times 1)$, no structural change of the CoPc hexagonal arrays was observed in the potential range between 0 and 1.0 V. Further, no structural change in the reconstructed surface was observed in this potential range. More measurements are needed to support this interpretation.

(2) CuPc Adlayers. The structure of a CuPc adlayer on Au(111) was further investigated. Figure 7a shows an STM image of CuPc arrays formed on Au(111) by immersion into a benzene solution saturated with CuPc for 1 h. The terrace was not fully covered with CuPc arrays; two regions, i.e., ordered and disordered phases, are seen. Under the highly ordered arrays of CuPc, reconstruction of Au(111) is clearly observed. Molecular features could not be discerned on the (1×1) region, probably because CuPc molecules were disordered. The structure of a CuPc adlayer formed on the reconstructed Au(111) gave a rectangular unit cell with the lattice parameter of 1.45 ± 0.05 nm, which is equal to that of CoPc on reconstructed Au(111). The CuPc arrays having a well-ordered square lattice on reconstructed Au(111) were consistently observed in the potential range between 0.2 and 0.9 V. Figure 7b shows a typical STM image of a CuPc adlayer formed on the Au(111)$-(1 \times 1)$ surface, which was acquired at 0.85 V in 0.1 M $HClO_4$. The CuPc adlayer was prepared by immersion for 22 h. It took a

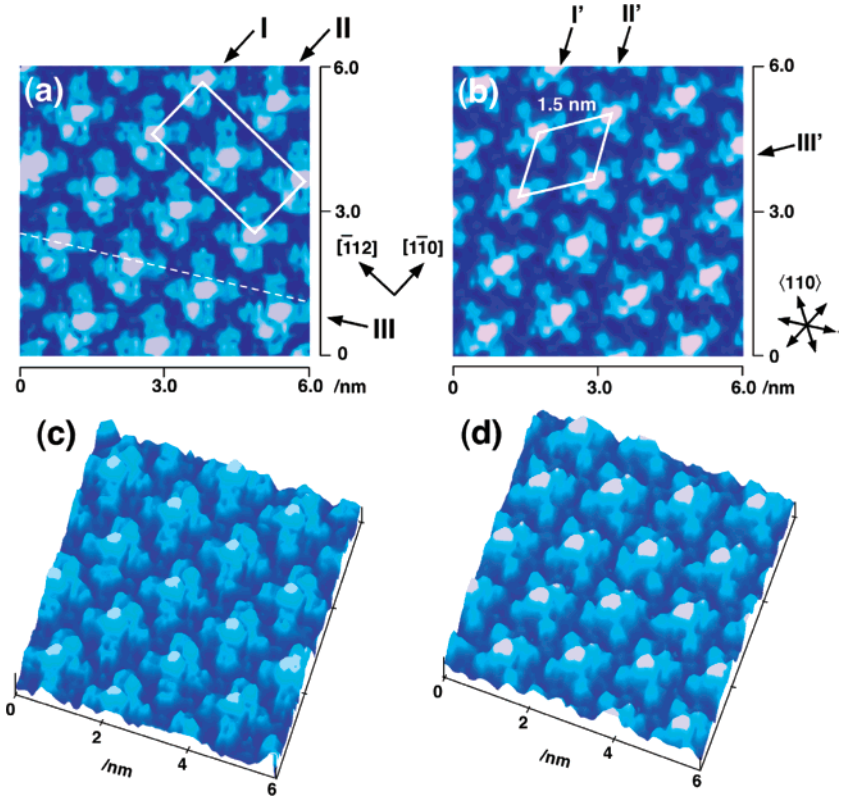

Figure 5. High-resolution STM images (6 × 6 nm^2) of domains labeled A and B in Figure 4 and height-shaded plots (c and d) of the CoPc adlayer on the Au(111)−(1 × 1) surface in 0.1 M $HClO_4$, acquired at 0.85 V versus RHE. The potentials of the tip and the tunneling currents were 0.45 V and 10 nA, respectively.

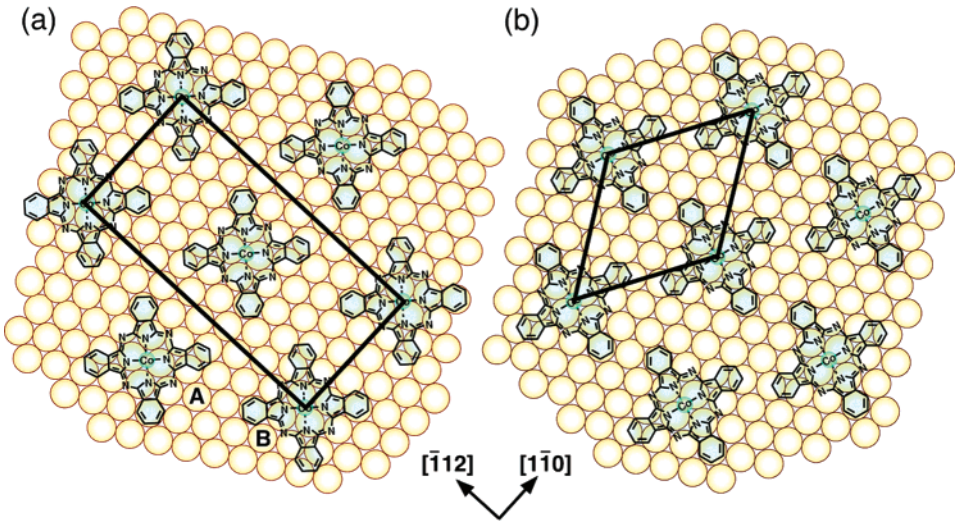

Figure 6. Proposed models for two CoPc adlayers formed on the Au(111)−(1 × 1) surface superimposed with *c*(5 × 6$\sqrt{3}$)*rect* (a) and (3$\sqrt{3}$ × 3$\sqrt{3}$)R30° unit cells (b).

longer time to form CuPc adlayers because of the low solubility of CuPc in benzene. Although some disordered areas were still seen, highly ordered molecular arrays were observed consistently on the terrace (Figure 7b). A typical domain size of CuPc was found to be 20 × 20 nm^2. In the image acquired in an area of 40 × 40 nm^2, two domains marked by A and B were found. Molecular rows between domains A and B cross each other at an angle of 90°. Molecular rows in domain A are aligned along the $\sqrt{3}$ direction of the Au(111) lattice, whereas those in domain B are aligned along the atomic direction of the Au(111) lattice. Two different domains, which are identical to those of CoPc, were also observed in CuPc adlayers formed on Au(111). It was found that regions A and B were composed of (3$\sqrt{3}$ × 3$\sqrt{3}$)R30° and *c*(5 × 6$\sqrt{3}$)*rect* adlattces, respectively. Because reconstructed rows of Au(111) were not seen under the present conditions, the CuPc adlayers shown in Figure 7b were formed on the Au(111)−(1 × 1). The hexagonal CuPc arrays on Au(111)−(1 × 1) revealed the same structure in the potential region between 0.15 and 0.95 V. A high-resolution STM image obtained in domain B forming *c*(5 × 6$\sqrt{3}$)*rect* is shown in Figure 8. Although the symmetry of CuPc adlayer is also *c*(5 × 6$\sqrt{3}$)*rect*, there is one difference between the STM image for CoPc in Figure 5a and that for CuPc in Figure 8: the center of CuPc is seen as a dark spot, whereas the cobalt ion in CoPc is bright. It is noteworthy that the brightness of the center spot in each molecule did not depend on the bias condition. Hipps

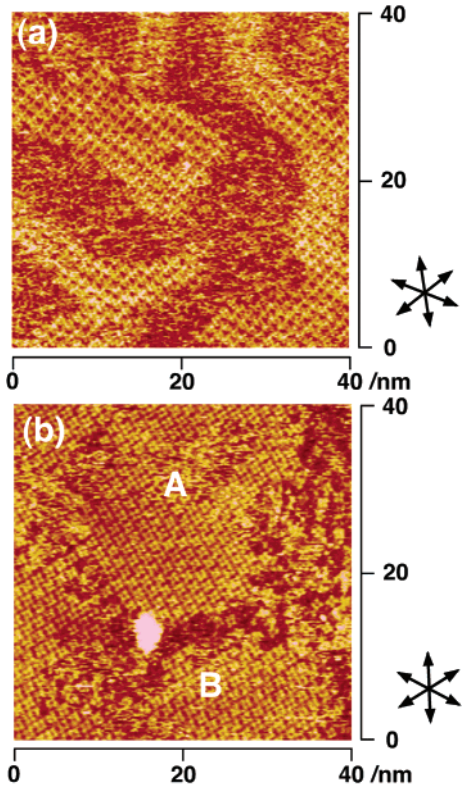

Figure 7. Large-scale (40 × 40 nm^2) STM images of a CuPc adlayer on reconstructed Au(111) (a) and Au(111)−(1 × 1) (b) surfaces acquired in 0.1 M $HClO_4$ at 0.85 V versus RHE. The potentials of the tip and the tunneling current were 0.45 V and 10 nA, respectively. The set of three arrows indicates the close-packed directions of the Au(111) substrate.

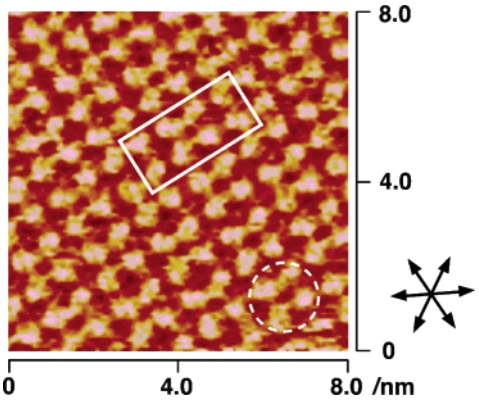

Figure 8. High-resolution STM image of a CuPc adlayer on the Au(111)−(1 × 1) surface in 0.1 M $HClO_4$, acquired at 0.85 V versus RHE. The potential of the tip and the tunneling current were 0.45 V and 10 nA, respectively. The set of three arrows indicates the close-packed directions of the Au(111) substrate.

and co-workers reported based on their experiments in UHV that the difference in brightness between the center metals of CoPc and CuPc was due to the difference in the mode of occupation of d orbitals.[12,13] The d orbital configuration of CoPc is d_{xz}^2, d_{yz}^2, d_{xy}^2, whereas that of CuPc is d_{xz}^2, d_{yz}^2, d_{xy}^2, $d_{z^2}^2$; that is, CoPc has a half filled d_{z^2} orbital.[12] In the case of CuPc, the center spot appears dark because the d orbital is filled, whereas the center spot of CoPc appears bright because the tunneling is mediated by the half filled d_{z^2} orbital between the Au surface and the tip.[12] A similar difference in the brightness of center metals was also reported for CoTPP and CuTPP on Au(111) in aqueous solution as described in our recent paper.[30]

Conclusions

By immersing a Au(111) substrate into a benzene solution saturated with CoPc or CuPc, we succeeded in preparing well-defined adlayers of CoPc and CuPc molecules on the Au(111) surface. It was found that the CoPc-modified Au(111) electrode enhanced the cathodic current for the electrocatalytic reduction of O_2 to H_2O_2. Packing arrangements and even the internal structure of each CoPc and CuPc molecule formed on Au(111) were determined by in situ STM in aqueous $HClO_4$. Adlayer structures of both CoPc and CuPc molecules depended on the immersion time. The structural transformation from square symmetry to hexagonal symmetry took place with an increase in immersion time. CoPc and CuPc molecules formed an incommensurate adlayer having a rectangular lattice with 1.45 nm on the reconstructed Au(111) surface, whereas commensurate adlayers of $c(5 \times 6\sqrt{3})rect$ and $(3\sqrt{3} \times 3\sqrt{3})R30°$ structures were found on the Au(111)−(1 × 1). The latter commensurate structures were newly found in solution for the first time in this study. The center cobalt ion in CoPc appeared as the brightest spot in the STM image, whereas the copper ion in CuPc appeared as a dark spot.

Acknowledgment. This research was partially supported by Grant-in-Aid for Science Research (A) (No. 12305055) from the Ministry of Education, Culture, Sports, Science and technology, Japan and by a Grant-in-Aid for the Center of Excellence (COE) Project, Giant Molecules and Complex Systems, 2003, and CREST-JST. The authors acknowledge Dr. Y. Okinaka for his assistance in writing this manuscript and Dr. J. Inukai of Tohoku University for his useful discussion.

References and Notes

(1) *Electron Transfer in Chemistry*; Balzani, V. Ed.; Wiley−VCH: New York, 2001; Vol. 3.
(2) Collman, J. P.; Wagenknecht, P. S.; Hutchison, J. E. *Angew. Chem., Int. Ed.* **1994**, *33*, 1537−1554 and references therein.
(3) *Molecular Electronics*; Jortner, J., Ratner, M., Eds.; IUPAC: Oxford, 1997.
(4) Guillaud, G.; Simon, J.; Germain, J. P. *Coord. Chem. Rev.* **1998**, *178*−*180*, 1433−1484.
(5) Jasinski, R. *J. Electrochem. Soc.* **1965**, *112*, 526−528.
(6) Alt, H.; Binder, H.; Sandstede, G. *J. Catal.* **1973**, *28*, 8−19.
(7) Savy, M.; Andro, P.; Bernard, C.; Magner, G. *Electrochim. Acta* **1973**, *18*, 191−197.
(8) Mho, S.-i.; Ortiz, B.; Park, S.-M.; Ingersoll, D.; Doddapaneni, N. *J. Electrochem. Soc.* **1995**, *142*, 1436−1441.
(9) Cárdenas-Jirón, G. I.; Gulppi, M. A.; Caro, C. A.; del Río, R.; Páez, M.; Zagal, J. H. *Electrochim. Acta* **2001**, *46*, 3227−3235 and references therein.
(10) Lippel, P. H.; Wilson, R. J.; Miller, M. D.; Wöll, C.; Chiang, S. *Phys. Rev. Lett.* **1989**, *62*, 171−174.
(11) Chizhov, I.; Scoles, G.; Kahn, A. *Langmuir* **2000**, *16*, 4358−4361.
(12) Lu, X.; Hipps, K. W.; Wang, X. D.; Mazur, U. *J. Am. Chem. Soc.* **1996**, *118*, 7197−7202.
(13) Hipps, K. W.; Lu, X.; Wang, X. D.; Mazur, U. *J. Phys. Chem.* **1996**, *100*, 11207−11210.
(14) Lu, X.; Hipps, K. W. *J. Phys. Chem. B* **1997**, *101*, 5391−5396.
(15) Barlow, D. E.; Hipps, K. W. *J. Phys. Chem. B* **2000**, *104*, 5993−6000.
(16) Lackinger, M.; Hietschold, M. *Surf. Sci.* **2002**, *520*, L619-L624.
(17) Strohmaier, R.; Ludwig, C.; Petersen, J.; Gompf, B.; Eisenmenger, W. *J. Vac. Sci. Technol. B* **1996**, *14*, 1079−1082.
(18) Qiu, X.; Wang, C.; Yin, S.; Zeng, Q.; Xu, B.; Bai, C.-L. *J. Phys. Chem. B* **2000**, *104*, 3570−3574.
(19) Xu, B.; Yin, S.; Wang, C.; Qiu, X.; Zeng, Q.; Bai, C.-L. *J. Phys. Chem. B* **2000**, *104*, 10502−10505.
(20) Lei, S.-B.; Wang, C.; Yin, S.-X.; Wang, H.-N.; Xi, F.; Liu, H.-W.; Xu, B.; Wan, L.-J.; Bai, C.-L. *J. Phys. Chem. B* **2001**, *105*, 10838−10841.
(21) Kunitake, M.; Batina, N.; Itaya, K. *Langmuir* **1995**, *11*, 2337−2340.
(22) Batina, N.; Kunitake, M.; Itaya, K. *J. Electroanal. Chem.* **1996**, *405*, 245−250.

(23) Kunitake, M.; Akiba, U.; Batina, N.; Itaya, K. *Langmuir* **1997**, *13*, 1607−1615.
(24) Ogaki, K.; Batina, N.; Kunitake, M.; Itaya, K. *J. Phys. Chem.* **1996**, *100*, 7185−7190.
(25) Sashikata, K.; Sugata, T.; Sugimasa, M.; Itaya, K. *Langmuir* **1998**, *14*, 2896−2902.
(26) Wan, L.-J.; Shundo, S.; Inukai, J.; Itaya, K. *Langmuir* **2000**, *16*, 2164−2168.
(27) Itaya, K. *Prog. Surf. Sci.* **1998**, *58*, 121−248.
(28) Tao, N. J.; Cardenas, G.; Cunha, F.; Shi, Z. *Langmuir* **1995**, *11*, 4445−4448.
(29) Tao, N. J. *Phys. Rev. Lett.* **1996**, *76*, 4066−4069.
(30) Yoshimoto, S.; Tada, A.; Suto, K.; Narita, R.; Itaya, K. *Langmuir* **2003**, *19*, 672−677.
(31) Scudiero, L.; Barlow, D. E.; Hipps, K. W. *J. Phys. Chem. B* **2000**, *104*, 11899−11905.
(32) Scudiero, L.; Barlow, D. E.; Mazur, U.; Hipps, K. W. *J. Am. Chem. Soc.* **2001**, *123*, 4073−4080.
(33) Yoshimoto, S.; Narita, R.; Wakisaka, M.; Itaya, K. *J. Electroanal. Chem.* **2002**, *532*, 331−335.
(34) Clavilier, J.; Faure, R.; Guinet, G.; Durand, R. *J. Electroanal. Chem.* **1980**, *107*, 205−209.
(35) Honbo, H.; Sugawara, S.; Itaya, K. *Anal. Chem.* **1990**, *62*, 2424−2429.
(36) Yoshimoto, S.; Narita, R.; Itaya, K. *Chem. Lett*. **2002**, 356−357.
(37) Yoshimoto, S.; Narita, R.; Tsutsumi, E.; Matsumoto, M.; Itaya, K.; Ito, O.; Fujiwara, K.; Murata, Y.; Komatsu, K. *Langmuir* **2002**, *18*, 8518−8522.
(38) Kolb, D. M.; Schneider, J. *Electrochim. Acta* **1986**, *31*, 929−936.
(39) Dretschkow, Th.; Dakkouri, A. S.; Wandlowski, Th. *Langmuir* **1997**, *13*, 2843−2856.